Optimum LED semiangle and the receiver FOV selection for Indoor VLC System with Human Blockages

Anand Singh[+], Anand Srivastava[+], and Vivek Ashok Bohara[+]

[+]Wirocomm Research Group, [+]Department of Electronics & Communication Engineering
[+]IIIT-Delhi, New Delhi, India, 110020
Email: anandsi@iiitd.ac.in

In this paper, we have determined the optimum pair of light-emitting diode (LED) semiangle and the receiver field-of-view (FOV) in the presence of human blockages for indoor visible light communication (VLC) system. Firstly, we have calculated the optimum value of LED semiangle and the receiver FOV independently, keeping others constant. Secondly, we have jointly optimized both the LED semiangle and the receiver FOV. In the analysis, both LoS and NLoS up to the second-order have been considered. We have also incorporated the reflections from the human body, essentially the skin and the clothes, in the analysis as it impacts the received power. In order to obtain the optimum value of the LED semiangle and the receiver FOV, we have used the quality factor (Q) as a performance metric. In addition, the analytical expression for the achieved quality factor is derived for both single variable and joint optimization formulation. Results shows that with 2 and 5 blockages, the optimum pair using single and joint optimization is $(63^\circ, 65^\circ)$ and $(63^\circ, 70^\circ)$ for a separation distance of D_1 = 40 cm and $(65^\circ, 70^\circ)$ and $(65^\circ, 75^\circ)$ for D_2 = 20 cm respectively which provide the highest quality factor with minimum delay spread shown. Furthermore, the optimization analysis can also be mapped to different room sizes and LED placement, with static and dynamic blockages inside the room.

***Index Terms*—Visible light communication (VLC), Field-of-View (FOV), LED semiangle, Human blockage, Matern hardcore point process (MHCP).**

I. INTRODUCTION

The growing demand for a higher data rate is the foremost cause of accelerating research to reduce the radio frequency (RF) wireless communication burden. Furthermore, the demand is much more severe in indoor communication where the maximum data usage occurs [1]. Visible light communication (VLC) is an optical wireless communication technology that can satisfy the high capacity demand in an indoor scenario [2], [3]. An indoor VLC system's performance depends on various factors such as light-emitting-diode (LED) semiangle, receiver field-of-view (FOV), wall reflections, and the obstacles present in the room. In [4], authors optimize the Lambertian order of LEDs in order to increase the minimum received power with LoS links. However, the effect of NLoS links is not considered. In [5], authors proposed an evolutionary algorithm-based optimization to modify the optical intensity of LED transmitters for reducing the signal power fluctuation. Despite the fact that the effect of obstacles inside the room is not included in the analysis. Similarly, in [6] a mathematical design model to maximize the power due to line-of-sight (LoS) link, as well as a practical measurement for an indoor diffuse cellular VLC system only with an LoS channel, is proposed. It is shown that using holographic light shaping diffusers (LSDs) with suitable angles and uniform power distribution can be obtained, thus increasing the coverage area in an indoor VLC environment. Further, authors in [7] studied the VLC channel with the random shadowing due to furniture present in the room to only with LoS link. It is shown that the decrease in normalized received power for an indoor VLC system follows the Rayleigh distribution. Furthermore, in [8] authors presents a novel channel model for indoor VLC is proposed in which LEDs are adopted to make a detection of the obstacle by beam steering. Then, the obstacle is described as a convex hull. Further, Chen et al., in [9] propose a modified Monte Carlo ray-tracing method is proposed to account for both the specular and diffusive reflections in calculating VLC channel impulse response at a given location. The effect of blockages in the system has not been included, affecting the VLC channel impulse response. In [10] and [5], the authors compare the channel characteristics of both the simplified point-source model (single LED) and six practical cases having various numbers of LEDs. Their results show that the deviations in terms of the channel's optical path loss (OPL) and its bandwidth and the channel's delay spread are steadily increased upon increasing the number of LEDs of each transmitter until LEDs spread almost over the entire ceiling. Moreover, none of the works listed above have analyzed the effect in indoor VLC system parameters in the presence of static and dynamic obstacles.

In the earlier analysis of the VLC system, they avoid the impact of human blockages in the room, which will affect the system parameter values due to shadowing. Also, they do not study the impact of several practical system parameters like the order of reflections from the wall and human body reflection in the analysis in order to get the optimum values of VLC parameters. The motivation behind this work is to find out the optimum pair of LED semiangle, and the receiver FOV in the presence of human blockages, including reflections from the walls up to two-point and also the reflections from the human body [11] which can contribute to received power. To analyze the impact of human blockages in indoor VLC systems performance, we have employed a Matern hardcore point process (MHCP) model to realize the static blockages [12].

Our work aims to bridge these gaps in the literature and has

some novel contributions as outlined below:

1) This work optimizes the LED semiangle and the receiver FOV for an indoor VLC system in the presence of human blockages for 4 LEDs in a rectangular configuration in order to provide high-quality factor and minimum delay spread across the room.
2) In the analysis of quality factor inside the room, wall reflection up to second-order and reflections from the human body and the clothes are considered.
3) A Joint optimization framework along with single variable optimization have been proposed to provide us the optimum value of VLC parameter (LED semiangle and receiver FOV) considering the impact of human blockages.
4) Further, we investigate the effect of the number of blockages on received quality factor with respect to varying FOV and LED irradiance angles and suggest optimum range (FOV and LED semiangle) of operation subject to the number of blockages inside the room.
5) Moreover, We also analyze the trade-off between the required quality factor and the delay spread across the room with respect to the number of blockages, LED semiangle, and the receiver FOV.

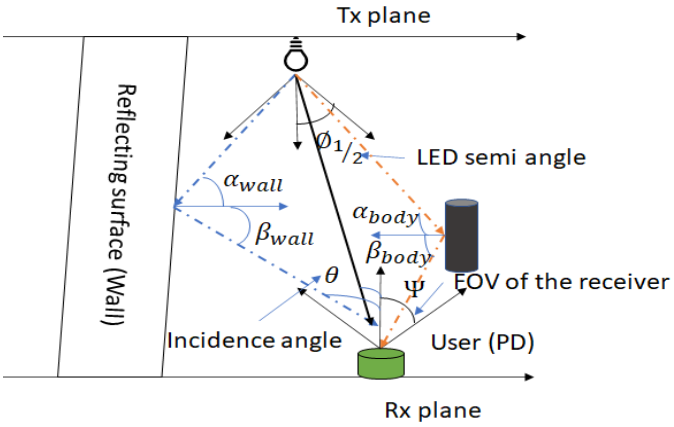

Fig. 1. System model

II. System Model

In this section, we discuss the system model of an indoor VLC system with human blockages inside. We have used the Matern type-II process to distribute the location of the blockages in a plane with an intensity of λ_B respectively. The blockages are assumed to be cylindrical with radius r and the height h_B as shown in Fig.1. For the proposed system model, two types of blockages of having radius $r_1 = 20$ cm, $r_2 = 40$ cm which are equivalent to varying sizes of humans with a minimum separation distance of $D_1 = 40$ cm, $D_2 = 20$ cm have been considered. Also, the surface of a human body exposed to light propagation is composed of two main parts, the skin, and the clothes, and their ρ values vary according to the light wavelength. We have used the mean human body reflection value of 0.51 mentioned in [11]. The receiver plane is considered to be 0.85m above the floor. Both LOS and NLOS paths are considered [13]. The receiver plane is divided into 25×25 sub-region to cover the whole room for analysis.

In the following subsections, we discuss in detail the multipath VLC channel, the impact of the human body, and the modeling of human blockages.

A. VLC Channel Model

In this paper, we have used a multipath VLC channel model with reflection up to second order. Lambert radiator is a typical radiation model that can model the LED light source in VLC. It has also been pointed out in [1] that the Lambertian model can accurately reproduce the LoS and non-line-of-sight (NLoS) luminous intensity pattern of the LEDs. Thus, the VLC channel response is a sum of both the LoS path (direct path between the LED and the user) and the NLoS path reflecting from the walls as shown in Fig. 1.

The channel gain of LoS component H_{LoS}, is given as:

$$H_{LoS} = \begin{cases} \frac{(m+1)A}{2\pi D^2} \cos^m(\phi) T_s g(\psi) \cos(\theta) & 0 \le \Psi \le \Psi_c, \end{cases} \tag{1}$$

where m represents Lambertian order defined as:

$$m = \frac{-ln(2)}{ln(cos(\Phi_{\frac{1}{2}}))} \quad . \tag{2}$$

In (1), A is the physical area of the PD, D_d is the distance between the VLC transmitter and the receiver, θ is the angle of incidence to the PD from LED, ϕ is the LED angle of irradiance, ψ_c is the receiver FOV, $T_s(\psi)$ is the gain of the optical filter, and $g(\psi)$ is the gain of the optical concentrator given as:

$$g(\psi) = \begin{cases} \frac{n^2}{\sin^2(\Psi_c)}, & 0 \le \Psi \le \Psi_c, \end{cases} \tag{3}$$

where n is the refractive index of optical concentrator and $\phi_{\frac{1}{2}}$ is LED semi angle. The NLoS channel gain is defined as:

$$H_{NLoS}^{wall} = \begin{cases} \frac{\rho_1 (m+1) A}{2\pi D_1^2 D_2^2} \cos^m(\phi) T_s(\psi) g(\psi) \\ \qquad \cos(\alpha_{wall}) \cos(\beta_{wall}) \\ \qquad 0 \le \Psi \le \Psi_c \quad , \end{cases} \tag{4}$$

Here α_{wall} and β_{wall} are the incidence and reflectance angle non line of sight link make with reflecting surface (wall) have reflection coefficient ρ. D_1, D_2 are the distance travelled by NLoS link to reach user from the wall.

B. Impact of human body

We consider geometrical models, one in 2D corresponding to the profile of a generic human body as a cylinder with a height of 180 cm and width of 20 cm and 40 cm, respectively.

As discussed in the above subsection I-B, firstly, we realize the human blockages with the help of the MHCP process. Then for each realization, we calculate the reflections from the human body to the PD using the ray-tracing model [14].

So the received power, including reflections from the human body can be written as:

$$H_{NLoS}^{body} = \begin{cases} \frac{\rho_2(m+1)A}{2\pi D_3^2 D_4^2}\cos^m(\phi)T_s(\psi)g(\psi).. \\ \qquad \cos(\alpha_{body})\cos(\beta_{body}) \\ \qquad 0 \le \Psi \le \Psi_c \ , \end{cases} \tag{5}$$

Here α_{body} and β_{body} are the incidence and reflectance angle NLoS link make with reflecting surface (wall) have reflection coefficient ρ. D_3, D_4 are the distance travelled by NLoS link to reach the user from the blockages.

For a given transmission power (P_T), the total received power using multiple LEDs, including diffused paths through the walls and the human body can be obtained as:

$$P_r = \sum_{i=1}^{N}\left[P_T H_{LoS} + \sum_{k=1}^{K} P_T H_{NLoS}^{wall} + \sum_{j=1}^{M} P_T H_{NLoS}^{body}\right] . \tag{6}$$

Here N is the total number of transmitting LEDs, M are the expected number of human blockage realized using MHCP process, and the total power is obtained by ingratiating both LoS the NLoS link across the room.

C. Modeling of human blockages using MHCP

In this subsection, we have characterized the homogeneous blockage process having radius r_B using MHCP. First, a parent Poisson point process is generated to realize the locations of human blockages in a 2-D plane. A random point or mark is associated with each human blockage, and a point of the parent Poisson process is deleted if there is another mark within the hardcore distance of δ. The intensity of the resulting process is $\lambda_{B1} = \frac{1-\exp(\lambda_p \pi \delta^2)}{\pi\delta^2}$, where λ_p is the intensity of the parent point process [15]. The link between two nodes located at a distance d_B from each other is blocked if an element of the point process falls in the shadow region of the blockage. The probability that the center of at least one blocking object falls in the shaded the area can be calculated using the void probability $P_B(d) = 1 - \exp\left(-2\lambda_{B1} d_B r_B^2\right)$ where λ_{B_1} is the blockage intensity having same radius and r_B is the blockage radius which can be either r_1 or r_2.

III. VLC Parameter Optimization

This section discusses the optimization framework for the LED semiangle and the receiver FOV in the presence of human blockages. Here, our goal is to optimize the power at the receiver in the presence of human blockages considering second-order reflections from the wall and the reflections from the human body. Therefore, we define Quality factor as a performance metric, which is defined as the ratio of average received power to the variance of the received power:

$$Q = \frac{\bar{P_{rec}}}{2\sqrt{Var(P_{rec})}} \tag{7}$$

where $\bar{P_{rec}}$ is the average received power across the room and $Var(P_{rec})$ is the variance of received power across the room.

The average received power $\bar{P_{rec}}$ can be defined as:

$$\bar{P_{rec}} = E\left[P_{rec}\right] = \frac{1}{A_{floor} \times N}\int_x \int_y P_{rec} dxdy \tag{8}$$

where $A_{floor} = x \times y$ is the indoor room floor area which we have divided into number of grids, x and y represents the length and width of the room respectively.

The variance $Var(P_{rec})$ of the received power across the room can be defined as:

$$\begin{aligned} Var(P_{rec}) &= \left[E\left[P_{rec}^2\right] - \left[E\left(P_{rec}\right)\right]^2\right] \\ &= \frac{1}{A_{floor}}\int_x \int_y \left[P_{rec}^2 - \left(\bar{P_{rec}}\right)^2\right] dxdy \end{aligned} \tag{9}$$

Using (7), (8) and (9) the quality factor can be expressed as:

$$Q = \frac{\frac{1}{A_{floor}\times N}\int_x \int_y P_{rec} dxdy}{2\sqrt{\frac{1}{A_{floor}}\int_x \int_y \left[P_{rec}^2 - \left(\bar{P_{rec}}\right)^2\right] dxdy}} \tag{10}$$

A. FOV optimization

In this section, we describe the optimization of the FOV of the receiver such that the optical power detected on the receiver plane has a high average value and low spatial variations. For the FOV optimization, we have expressed the quality factor as a function of the FOV Ψ_c of the receiver. It can be observed from (7) that the quality factor is a function of the received power and variance, which we can write as a function of receiver FOV.

The average receive power $\bar{P_{rec}}(\Psi_c)$ as a function of receiver FOV Ψ_c:

$$\bar{P_{rec}}(\Psi_c) = \frac{1}{A_{floor} \times N}\int_x \int_y P_{rec}(\Psi_c) dxdy, \tag{11}$$

where $P_{rec}(\Psi_c)$ can be expressed using (3), (4) and (5):

$$\begin{aligned} P_{rec}(\Psi_c) &= \frac{(m+1)AP_T}{2\pi D^2}\cos^m(\phi)T_s g(\psi)\cos(\theta) \\ &= \frac{(m+1)AP_T}{2\pi\left[\sqrt{(x_R - x_T)^2 + (y_R - y_T)^2 + h^2}\right]} \\ &\quad \cos^m(\phi)T_s\cos(\theta)\frac{n^2}{\sin^2(\psi_c)}. \end{aligned} \tag{12}$$

where (x_T, y_T), (x_R, y_R) are the transmitter and receiver location coordinates, respectively and h is the height of the receiver plane from transmitter plane.

Putting the value of $P_{rec}(\Psi_c)$ in (11) the average receive power $\bar{P_{rec}}(\Psi_c)$ as a function of receiver FOV Ψ_c:

$$\begin{aligned} \bar{P_{rec}}(\Psi_c) &= \frac{1}{A_{floor} \times N}\int_x \int_y \\ &\quad \frac{(m+1)AP_T}{2\pi\left[\sqrt{(x_R - x_T)^2 + (y_R - y_T)^2 + h^2}\right]} \\ &\quad \cos^m(\phi)T_s\cos(\theta)\frac{n^2}{\sin^2(\psi_c)} dxdy, \end{aligned} \tag{13}$$

Similarly the variance of the received power can be expressed as a function of receiver FOV Ψ_c:

$$Var(\Psi_c) = E\left[P_{rec}^2(\Psi_c)\right] - \left[E\left(P_{rec}(\Psi_c)\right)\right]^2 = \frac{1}{A_{floor}} \int_x \int_y \left(P_{rec}^2(\Psi_c) - \left(\bar{P_{rec}}(\Psi_c)\right)^2\right) dxdy. \tag{14}$$

Finally, the quality factor Q can be expressed as a function of receiver FOV Ψ_c:

$$Q(\Psi_c) = \frac{\bar{P_{rec}}(\Psi_c)}{2\sqrt{Var(\Psi_c)}}, \tag{15}$$

For optimal solution to find the maximum value of quality factor subject to the receiver FOV Ψ_c

$$\frac{dQ(\Psi_c)}{d(\Psi_c)} = 0, \tag{16}$$

Solving the above optimality condition (16), the optimality equation subject to receiver FOV can be written as:

$$\frac{dP_{rec}(\Psi_c)}{d(\Psi_c)}\sqrt{Var(\Psi_c)} + \frac{d\sqrt{Var(\Psi_c)}}{d(\Psi_c)} P_{rec}(\Psi_c) = 0. \tag{17}$$

Now we can calculate the values of $P_{rec}(\Psi_c)$, $Var(\Psi_c)$, $\frac{dP_{rec}(\Psi_c)}{d(\Psi_c)}$ and $\frac{d\sqrt{Var(\Psi_c)}}{d(\Psi_c)}$ numerically bu putting the value of VLC system parameter in the table I.

B. LED semiangle optimization

In this section, the optimization of LED semiangle in the presence of human blockage, keeping the FOV of the receiver constant, has been proposed. In the analysis, the wall reflection up to second-order has been considered. Again the quality factor is considered as a performance metric. Here we are maximizing the quality factor at the receiver subject to LED semiangle.

We have expressed quality factor Q as a function of LED semiangle Φ, which can be defined as:

$$Q(\Psi_c) = \frac{\bar{P_{rec}}(\Phi)}{2\sqrt{Var(\Phi)}} \tag{18}$$

By using optimality condition $\frac{dQ(\Psi_c)}{d(\Psi_c)} = 0$, we have obtained the LED semiangle optimal equation as:

$$\frac{dP_{rec}(\Phi)}{d(\Phi)}\sqrt{Var(\Phi)} + \frac{d\sqrt{Var(\Phi)}}{d(\Phi)} P_{rec}(\Phi) = 0. \tag{19}$$

Now we can calculate the values of $P_{rec}(\Phi)$, $Var(\Phi)$, $\frac{dP_{rec}(\Phi)}{d(\Phi)}$ and $\frac{d\sqrt{Var(\Phi)}}{d(\Phi)}$ numerically bu putting the value of VLC system parameter in the table I.

C. Joint Optimization

In this subsection, we describe the optimization of both LED semiangle and the receiver FOV subject to the maximization of the quality factor. The optical power detected on the receiver plane has a high average value and low spatial variations. Therefore, we first calculate the received power and the variance of the received power as a function of both the LED semiangle Φ and the receiver FOV Ψ_c jointly.

The quality factor Q as a function of LED semiangle and the receiver FOV jointly can be expressed as:

$$Q(\Psi_c, \Phi) = \frac{\bar{P_{rec}}(\Psi_c\Phi)}{2\sqrt{Var(\Psi_c\Phi)}} \tag{20}$$

The optimal value of both LED semiangle and the receiver FOV can be calculated using optimality condition $\frac{dQ(\Psi_c,\Phi)}{d(\Psi_c,\Phi)} = 0$.

$$\frac{\partial\left(\frac{\partial P_{rec}(\Psi_c,\Phi)}{\partial(\Psi_c)}\sqrt{Var(\Psi_c\Phi)} + \frac{\partial\sqrt{Var(\Psi_c\Phi)}}{\partial(\Psi_c)} P_{rec}(\Psi_c\Phi)\right)}{\partial(\Phi)} = 0. \tag{21}$$

TABLE I
SYSTEM MODEL PARAMETERS

Parameter	**Value**
Room size	5 m × 5 m × 3 m
LED transmitted power	200 mw
Refractive index n	1.5
Optical filter gain T_s	1
Wall reflection ρ_1	0.8
Human body reflection ρ_2	0.51
LED semiangle	60°
Receiver plane above the floor (h_R)	0.85 m
Receiver elevation	90°
Receiver active area	1 cm^2
Field of views (FOVs) of receiver	60°.
Blockage radius (r_1 and r_2)	20 cm & 40 cm
Height of the blockage (h_B)	180 cm
Responsivity ($\mathcal{R}$)	0.5 $\frac{A}{W}$
Signal bandwidth B_s	10 MHz
Noise bandwidth factor I_2	0.562
Background current I_{bg}	100 μA

IV. RESULTS AND DISCUSSION

This section presents and discusses the results obtained using simulation in MATLAB® environment in order to increase the value of quality factor subject to human blockages inside the room. The transmitter configurations of 4 LEDs in a rectangular geometry are considered. The locations and the orientations of the VLC transmitters and the receiver are provided in Table I.

A. VLC channel gain as a function of LED semi angle and receiver FOV

Fig. 2(a) and Fig. 2(b) shows the variation in VLC channel gain at the receiver FOV of 70° and 30° respectively. In both the case the LED semiangle considered is 15°, 30°,45° and 60°. We can see that the VLC channel gain is maximum at the lower values of LED semiangle (Φ) and FOV (Ψ_c), it starts decreasing with increasing value of Φ and Ψ_c.

It is due to the fact that the VLC channel is a cosine function of Φ and Ψ_c. We can also see that the VLC channel gain decreases as the distance to the LED and PD increases. As in the practical system, there will be obstacles inside the room. The VLC channel gain value will deteriorate due to

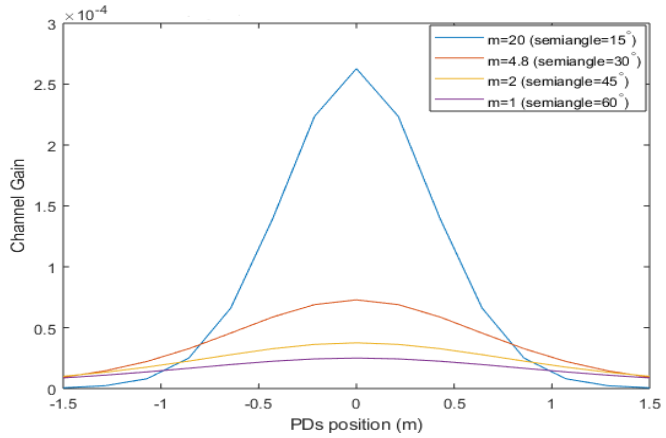

(a) Channel gain as a function of LED semi angle with FOV = 70^0

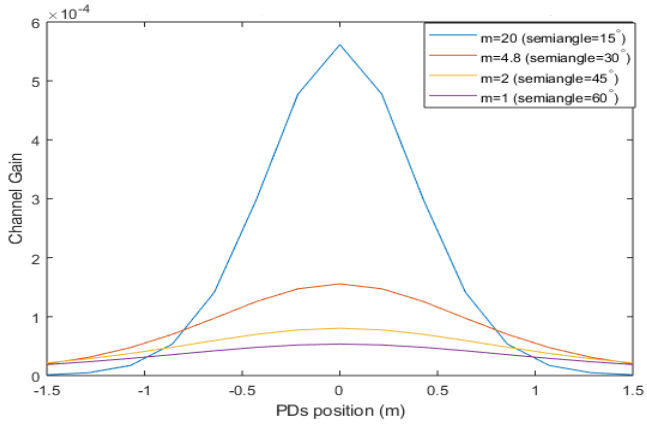

(b) Channel gain as a function of LED semi angle with FOV = 40^0

Fig. 2. Variation in VLC Channel gain as a function of PD's position

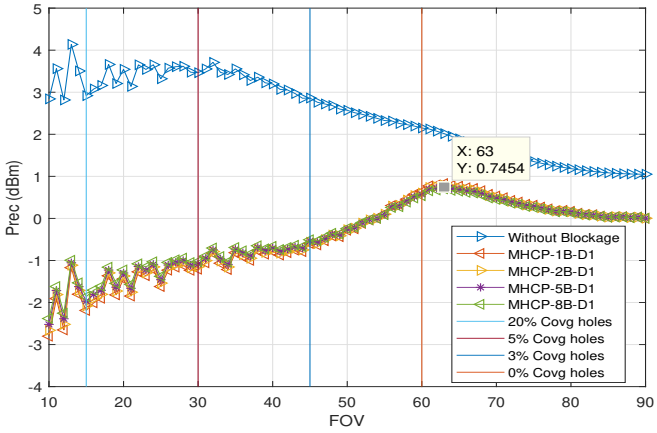

(a) Received power versus FOV with D1 = 40 cm

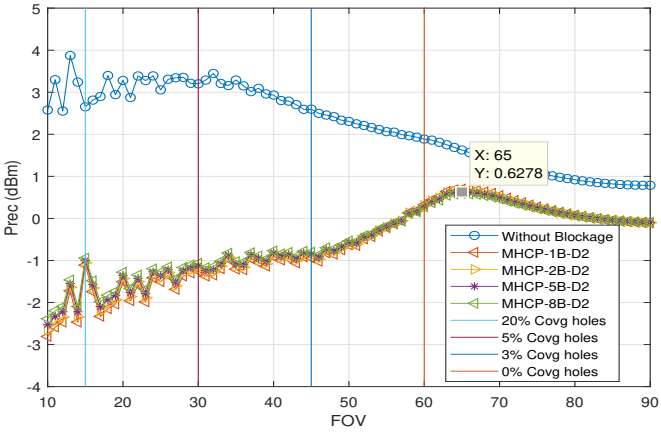

(b) Received power versus FOV with D2 = 20 cm

Fig. 3. Effect of varying FOV and the separation distance between the blockages on the received power

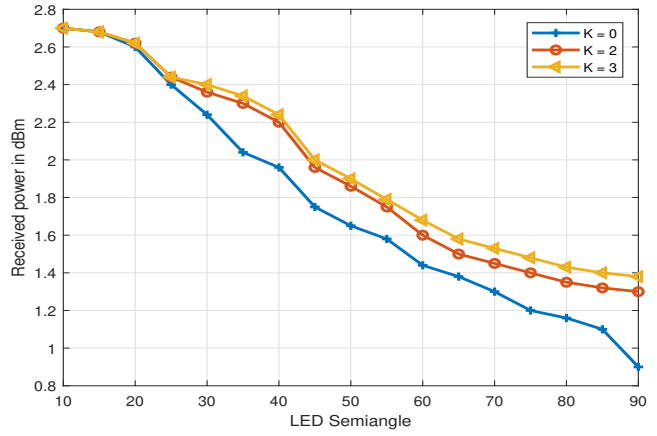

(a) Average received as function of LED semi angle with FOV = 60^0

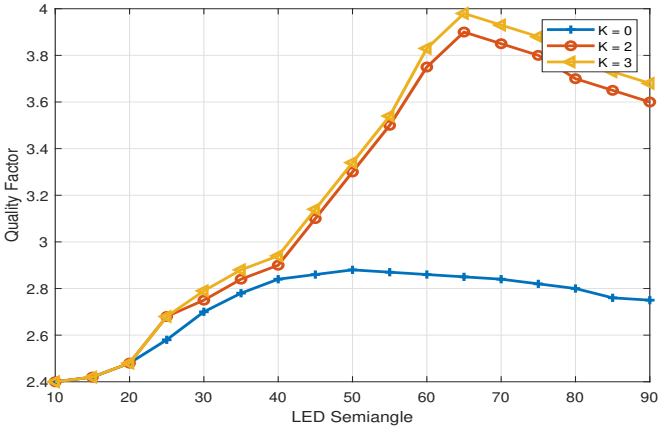

(b) Quality factor as a function of LED semi angle

Fig. 4. Effect of varying LED semiangle on received power and the quality factor

shadowing, so it is essential to get the optimum pair of Φ and Ψ_c, which will give us better performance across the room.

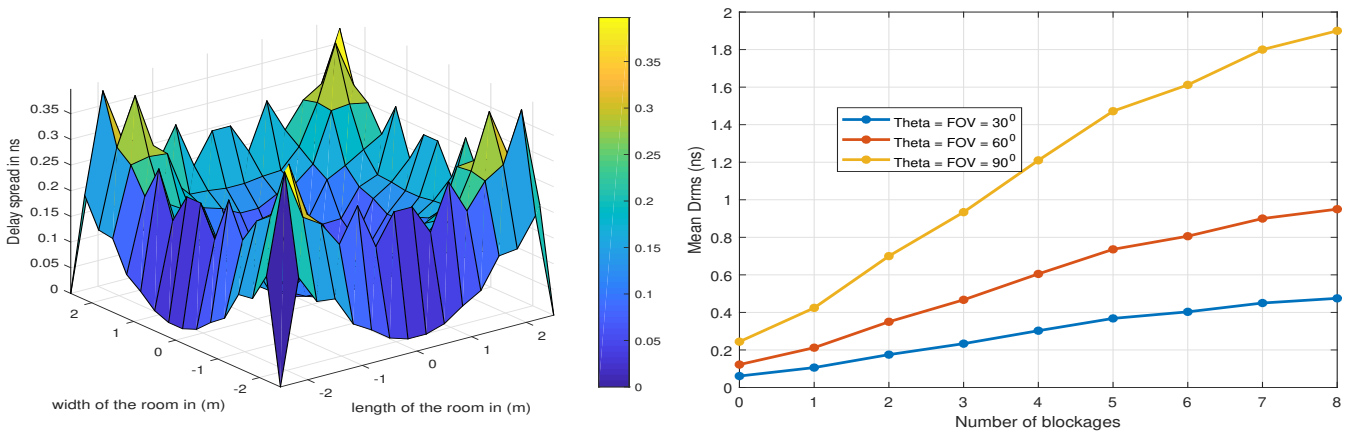

(a) Delay spread across the room without blockage

(b) Delay spread with blockage

Fig. 5. Delay spread Comparison without and with blockage

TABLE II
QUALITY FACTOR AND DELAY SPREAD PERFORMANCE WITH RESPECT TO PROPOSED OPTIMIZATION TECHNIQUES

Blockage	FOV (opt)	Q (FOV)	Theta (opt)	Q (Theta)	Delay Spread	Joint optimization	Q (Joint)	Delay spread (Joint)
D1-2B	63	8.05	65	8.50	0.25 ns	(63,65)	9.05	0.17 ns
D1-5B	63	7.52	70	8.06	0.40 ns	(63,70)	8.35	0.21 ns
D2-2B	65	6.09	70	7.11	0.70 ns	(65,70)	7.50	0.38 ns
D2-5B	65	5.21	75	2.25	5.54 ns	(65,75)	6.15	0.78 ns

B. Average Received power with varying FOV in the presence of blockage

Fig. 3(a) and 3(b) show the average received power as a function of varying receiver FOV. For without blockage case, as the receiver FOV increases, the average power decreases and becomes constant at the higher value of FOV. However, for with blockage case, the average power first increases, then after achieving its maximum value, it starts decreasing for different blockage densities and minimum separation among them. Because of blockage, the user will be in shadow, so it requires a wider FOV to get the power from other LEDs that are not in shadow. Also, wider FOV capture more and more NLoS signals. It can be observed that for a specific minimum separation distance, we are getting a particular value FOV where the average power is maximizing, like for separation distance of $D_1 = 40$ cm, the optimum FOV value is 63° for all the blockage densities. While for the minimum separation distance of $D_2 = 20$ cm, the optimum value of FOV is 65° for all the blockage density.

It can be concluded that in the presence of blockage, the optimum value of FOV varies as a function of blockage density and the separation distance between them. The optimum FOV value is lower for the larger separation distance due to the non-clustering of blockages because of broader spacing between them. On the other hand, as the minimum separation distance among them decreases, it results in the clustering of blockage. Therefore, it requires wider FOV to increase average power across the room.

C. Average Received power and the received quality factor with varying LED semiangle

Fig. 4(a) and 4(b) show the average received power and the quality factor as a function of LED semiangle, keeping the receiver FOV fixed at 60°. Here in the analysis, reflections of up to second-order from the wall have been considered. In Fig. 4 $K = 0$ means only the LoS link, $K = 1$ means LoS and first-order NLoS link, and $K = 2$ means LoS with second-order reflection.

As the LED semiangle value increases, the average received power and power decreases as shown in Fig. 4(a). Compared to only LoS links, the average received power loss for the case that considers both LoS and NLoS is less. Therefore, the average received power should be maximum for the uniform quality of service, and the variance should be minimum. To evaluate the same, we have plotted the quality factor (Q) (see (7)) in Fig. 4(b) as it includes both averages received power and variance of the power in the analysis. It can be seen from Fig. 4(b) as the value of LED semiangle increases initially, the quality factor increases and achieve its maximum value. For the higher values of LED semiangle, it starts decreasing. It can be seen that the quality factor reaches its maximum value at the LED semiangle value of $\Phi = 65^\circ$.

D. Delay spread with and without blockage

Fig. 5(a) shows the delay spread profile without any blockages across the room in which delay spread ranges from 0 ns to 0.35 ns. It can be observed that the delay spread is minimum in the center of the room and increasing towards the corner of the room because, at the corners, most of the received power

is due to NLoS links. Fig.5(b) shows the mean RMS delay spread as a function of a number of blockages in the room subject to different receiver FOV and LED semiangle values. For each case, the mean RMS delay spread increases with the increasing value of blockages, which is intuitive because the number of blockages more and reflections will be there in the received power because the LoS component will be blocked due to shadowing. For the case of $\Phi = \Psi_c = 30^\circ$ in this case the mean RMS delay spread is ranging from 0.1 ns to 0.25 ns and for the case of $\Phi = \Psi_c = 60^\circ$ in this case the mean RMS delay spread is ranging from 0.15 ns to 0.9 ns similarly for the case of $\Phi = \Psi_c = 60^\circ$ in this case the mean RMS delay spread is ranging from 0.22 ns to 1.9 ns. We can say that for a larger pair of LED semiangle and receiver FOV, the delay spread is more because many NLoS links will be generated due to the wide LED semiangle. The same large number of NLoS links will be captured by the PDs, while for the smaller pair of LED semiangle, fewer NLoS links will be generated because of the small LED semiangle and less captured by the PD due to small FOV.

E. Quality factor and Delay spread trade-off

In this subsection, we have shown the trade-off between the received quality factor and delay spread as a function of the number of blockages in the room with respect to proposed optimization techniques. Table II shows the quality factor versus the number of blockages subject to proposed optimization methods. It can be seen that joint optimization (both FOV and LED semiangle optimization) provides us the best quality factor and minimum delay spread compared to single variable optimization LED semiangle and FOV optimization independently.

Table II shows the comparison of the proposed optimization techniques in terms of obtained quality factor and delay spread. Further, we have also shown the optimum pair of the receiver FOV and the LED semiangle for the respective configuration. For example, with two blockages with a separation distance of D_1 = 40 cm, the obtained optimum pair with single and joint optimization is $\Psi_c = 63^\circ$, $\Phi = 65^\circ$ and the respective quality factor value is 8.05 using single variable optimization and 9.05 using joint optimization. Similarly, for the case of 5 blockages, the obtained optimum pair with joint and single optimization is $\Psi_c = 63^\circ$, $\Phi = 70^\circ$ and the respective quality factor value is 8.06 using single variable optimization and 8.35 using joint optimization. Similarly, delay spread of single variable optimization for 2 and 5 blockages using joint optimization 0.17 ns and 0.21 ns for D_1 = 40 cm and 0.38 ns and 0.78 ns for D_1 = 20 cm. Thus, we can see that the proposed joint optimization technique gives us the best possible quality factor with minimum delay spread in blockages compared to single variable optimization and without optimization case.

V. CONCLUSION

In this paper, we present the optimum pair of LED semiangle and the receiver FOV in the presence of human blockages. The quality factor value is maximized to get the optimum value of LED semiangle with the receiver FOV. Further, We also show the effect of wall reflections and the reflection from the human body into the analysis. Additionally, the results demonstrate that optimized LED semiangle and FOV pair perform better than any other combination. It has also shown that it can also minimize the delay spread in trade-off with quality factor. So one can choose the respective LED semiangle and FOV pair based on their requirements. Furthermore, the given framework for dynamic blockage can be extended realization and different LED configurations. As per the user's requirement, we can suggest an optimum pair of VLC parameters that provide a uniform service across the room.

REFERENCES

[1] F. Miramirkhani and M. Uysal, "Channel modeling and characterization for visible light communications," *IEEE Photonics Journal*, vol. 7, no. 6, pp. 1–16, 2015.

[2] Z. Ghassemlooy, S. Arnon, M. Uysal, Z. Xu, and J. Cheng, "Emerging optical wireless communications-advances and challenges," *IEEE journal on selected areas in communications*, vol. 33, no. 9, pp. 1738–1749, 2015.

[3] M. D. Soltani, X. Wu, M. Safari, and H. Haas, "Bidirectional user throughput maximization based on feedback reduction in lifi networks," *IEEE Transactions on Communications*, vol. 66, no. 7, pp. 3172–3186, 2018.

[4] D. Wu, Z. Ghassemlooy, H. Le Minh, S. Rajbhandari, M.-A. Khalighi, and X. Tang, "Optimisation of lambertian order for indoor non-directed optical wireless communication," in *2012 1st IEEE International Conference on Communications in China Workshops (ICCC)*. IEEE, 2012, pp. 43–48.

[5] J. Ding, Z. Huang, and Y. Ji, "Evolutionary algorithm based power coverage optimization for visible light communications," *IEEE communications letters*, vol. 16, no. 4, pp. 439–441, 2012.

[6] D. Wu, Z. Ghassemlooy, H. LeMinh, S. Rajbhandari, and Y. Kavian, "Power distribution and q-factor analysis of diffuse cellular indoor visible light communication systems," in *2011 16th European Conference on Networks and Optical Communications*. IEEE, 2011, pp. 28–31.

[7] Z. Dong, T. Shang, Y. Gao, and Q. Li, "Study on vlc channel modeling under random shadowing," *IEEE Photonics Journal*, vol. 9, no. 6, pp. 1–16, 2017.

[8] X. Nan, P. Wang, L. Guo, L. Huang, and Z. Liu, "A novel vlc channel model based on beam steering considering the impact of obstacle," *IEEE Communications Letters*, vol. 23, no. 6, pp. 1003–1007, 2019.

[9] J. Chen and T. Shu, "Statistical modeling and analysis on the confidentiality of indoor vlc systems," *IEEE Transactions on Wireless Communications*, vol. 19, no. 7, pp. 4744–4757, 2020.

[10] J. Ding, Z. Xu, and L. Hanzo, "Accuracy of the point-source model of a multi-led array in high-speed visible light communication channel characterization," *IEEE Photonics Journal*, vol. 7, no. 4, pp. 1–14, 2015.

[11] C. Le Bas, S. Sahuguede, A. Julien-Vergonjanne, A. Behlouli, P. Combeau, and L. Aveneau, "Human body impact on mobile visible light communication link," in *2016 10th International Symposium on Communication Systems, Networks and Digital Signal Processing (CSNDSP)*. IEEE, 2016, pp. 1–6.

[12] A. Singh, G. Ghatak, A. Srivastava, V. A. Bohara, and A. K. Jagadeesan, "Performance analysis of indoor communication system using off-the-shelf leds with human blockages," *IEEE Open Journal of the Communications Society*, vol. 2, pp. 187–198, 2021.

[13] S. Rajagopal, R. D. Roberts, and S.-K. Lim, "IEEE 802.15. 7 visible light communication: modulation schemes and dimming support," *IEEE Communications Magazine*, vol. 50, no. 3, pp. 72–82, 2012.

[14] C. Le Bas, S. Sahuguede, A. Julien-Vergonjanne, A. Behlouli, P. Combeau, and L. Aveneau, "Impact of receiver orientation and position on visible light communication link performance," in *2015 4th International Workshop on Optical Wireless Communications (IWOW)*. IEEE, 2015, pp. 1–5.

[15] B. Matérn, *Spatial variation*. Springer Science & Business Media, 2013, vol. 36.